Research Article | Vol. 25, No. 16 | 7 Aug 2017 | OPTICS EXPRESS 19179
Optics EXPRESS

InGaN μLEDs integrated onto colloidal quantum dot functionalized ultra-thin glass

K. Rae,[1,*] C. Foucher,[1,] B. Guilhabert,[1] M. S. Islim,[2] L. Yin,[2] D. Zhu,[3] R. A. Oliver,[3] D. J. Wallis,[3,4,5] H. Haas,[2] N. Laurand,[1] and M. D. Dawson[1]

[1]*Institute of Photonics, Department of Physics, SUPA, University of Strathclyde, Glasgow, UK*
[2]*LiFi Research and Development Centre, Institute for Digital Communications, University of Edinburgh, UK*
[3]*Department of Materials Science and Metallurgy, University of Cambridge, Cambridge, UK*
[4]*Plessey semiconductors Ltd, Tamerton Road, Roborough, Plymouth, UK*
[5]*Centre for High Frequency Engineering, University of Cardiff, Cardiff, UK*
**Katherine.rae@strath.ac.uk*

Abstract: Red-, orange-, and green-emitting integrated optoelectronic sources are demonstrated by transfer printing blue InGaN μLEDs onto ultra-thin glass platforms functionally enhanced with II-VI colloidal quantum dots (CQDs). The forward optical power conversion efficiency of these heterogeneously integrated devices is, respectively, 9%, 15%, and 14% for a blue light absorption over 95%. The sources are demonstrated in an orthogonal frequency division multiplexed (OFDM) visible light communication link reaching respective data transmission rates of 46 Mbps, 44 Mbps and 61 Mbps.

OCIS codes: (230.3670) Light-emitting diodes; (230.5590) Quantum-well, -wire, and -dot devices; (060.4510) Optical communications.

References and links

1. J. K. Kim and E. F. Schubert, "Transcending the replacement paradigm of solid-state lighting," Opt. Express **16**(26), 21835–21842 (2008).
2. J. J. D. McKendry, D. Massoubre, S. Zhang, B. R. Rae, R. P. Green, E. Gu, R. K. Henderson, A. E. Kelly, and M. D. Dawson, "Visible-light communications using a CMOS-controlled micro-light- emitting-diode array," J. Lightwave Technol. **30**(1), 61–67 (2012).
3. H. Haas, L. Yin, Y. Wang, and C. Chen, "What is LiFi?" J. Lightwave Technol. **34**(6), 1533–1544 (2016).
4. S. Rajbhandari, J. J. D. Mckendry, J. Herrnsdorf, H. Chun, G. Faulkner, H. Haas, I. M. Watson, D. O. Brien, and M. D. Dawson, "A review of Gallium Nitride LEDs for multi-gigabit-per-second visible light data communications," Semicond. Sci. Technol. **32**, 1–44 (2016).
5. M. S. Islim, R. X. Ferreira, X. He, E. Xie, S. Videv, S. Viola, S. Watson, N. Bamiedakis, R. V. Plenty, I. H. White, A. E. Kelly, E. Gu, H. Haas, and M. D. Dawson, "Towards a 10 Gb/s orthogonal frequency division multiplexing-based visible light communication using a GaN violet micro-LED," Photonics Research **5**(2), A35–A43 (2017).
6. M. F. Leitao, J. M. M. Santos, B. Guilhabert, S. Watson, A. E. Kelly, M. S. Islim, H. Haas, M. D. Dawson, and N. Laurand, "Gb/s visible light communications with colloidal quantum dot color converters," IEEE J. Sel. Top. Quantum Electron. **23**(5), 1–10 (2017).
7. H.-S. Kim, E. Brueckner, J. Song, Y. Li, S. Kim, C. Lu, J. Sulkin, K. Choquette, Y. Huang, R. G. Nuzzo, and J. A. Rogers, "Unusual strategies for using indium gallium nitride grown on silicon (111) for solid-state lighting," Proc. Natl. Acad. Sci. U.S.A. **108**(25), 10072–10077 (2011).
8. T. Kim, K. Cho, E. K. Lee, S. J. Lee, J. Chae, J. W. Kim, D. H. Kim, J. Kwon, G. Amaratunga, S. Y. Lee, B. L. Choi, Y. Kuk, J. M. Kim, and K. Kim, "Full-color quantum dot displays fabricated by transfer printing," Nat. Photonics **5**(3), 176–182 (2011).
9. J. Justice, C. Bower, M. Meitl, M. B. Mooney, M. A. Gubbins, and B. Corbett, "Wafer-scale integration of group III–V lasers on silicon using transfer printing of epitaxial layers," Nat. Photonics **6**(9), 612–616 (2012).
10. A. De Groote, P. Cardile, A. Z. Subramanian, A. M. Fecioru, C. Bower, D. Delbeke, R. Baets, and G. Roelkens, "Transfer-printing-based integration of single-mode waveguide-coupled III-V-on-silicon broadband light emitters," Opt. Express **24**(13), 13754–13762 (2016).
11. D. Kang, B. Gai, B. Thompson, S. M. Lee, N. Malmstadt, and J. Yoon, "Flexible Opto-Fluidic Fluorescence Sensors Based on Heterogeneously Integrated Micro-VCSELs and Silicon Photodiodes," ACS Photonics **3**(6), 912–918 (2016).

#300911 https://doi.org/10.1364/OE.25.019179
Journal © 2017 Received 26 Jun 2017; revised 26 Jul 2017; accepted 27 Jul 2017; published 31 Jul 2017

Optics EXPRESS

12. B. Guilhabert, A. Hurtado, D. Jevtics, Q. Gao, H. H. Tan, C. Jagadish, and M. D. Dawson, "Transfer printing of semiconductor nanowires with lasing emission for controllable nanophotonic device fabrication," ACS Nano **10**(4), 3951–3958 (2016).
13. A. J. Trindade, B. Guilhabert, D. Massoubre, D. Zhu, N. Laurand, E. Gu, I. M. Watson, C. J. Humphreys, and M. D. Dawson, "Nanoscale-accuracy transfer printing of ultra-thin AlInGaN light-emitting diodes onto mechanically flexible substrates," Appl. Phys. Lett. **103**(25), 253302 (2013).
14. A. J. Trindade, B. Guilhabert, E. Y. Xie, R. Ferreira, J. J. D. McKendry, D. Zhu, N. Laurand, E. Gu, D. J. Wallis, I. M. Watson, C. J. Humphreys, and M. D. Dawson, "Heterogeneous integration of gallium nitride light-emitting diodes on diamond and silica by transfer printing," Opt. Express **23**(7), 9329–9338 (2015).
15. Z. L. Liau, "Semiconductor wafer bonding via liquid capillarity," Appl. Phys. Lett. **77**(5), 651–653 (2000).
16. B. Guilhabert, C. Foucher, A.-M. Haughey, E. Mutlugun, Y. Gao, J. Herrnsdorf, H. D. Sun, H. V. Demir, M. D. Dawson, and N. Laurand, "Nanosecond colloidal quantum dot lasers for sensing," Opt. Express **22**(6), 7308–7319 (2014).

1. Introduction

GaN-based light emitting diodes (LEDs) are key devices for solid-state lighting [1] and the emerging field of visible light communications (VLC) [2, 3]. In VLC, LEDs are rapidly intensity modulated to transmit data wirelessly but can still be used for illumination or display functions as the modulation is too rapid to be perceived by the human eye. This is an attractive technology for expanding the capacity of wireless networks. Data rates of 5 Gb/s and approaching 10 Gb/s in free space were recently achieved using, respectively, a blue [4] and a UV [5] emitting GaN micro-sized LED (μLED). This is a feat made possible by the >0.4 GHz modulation bandwidth of these μLEDs and by advanced data encoding schemes such as orthogonal frequency division multiplexing (OFDM).

Longer wavelengths and white light are typically obtained by color converting blue or UV LEDs with rare-earth phosphors. However, phosphors have long luminescent lifetimes (μs to ms) and do not have the high modulation bandwidths required for VLC. Colloidal quantum dots (CQDs), such as those based on II-VI semiconductors, are an attractive alternative because of their shorter luminescent lifetimes, hence faster response to modulation, and narrow emission linewidth. The latter feature is in contrast to the broad emission of phosphors, making CQDs superior for color purity and offering the prospect of wavelength division multiplexing. To date, CQDs have been demonstrated in VLC links at 300 Mb/s when incorporated in PMMA (poly(methyl methacrylate)) and have a 10-30 MHz intrinsic modulation bandwidth [6]. In these reports however, the CQD color-converters were either remotely excited by, or mechanically placed in contact with, a μLED with a bandwidth up to 150 MHz. In this report, μLEDs are directly integrated onto the CQD color converting structure by micro-transfer printing (μTP), offering electronically-interfaced excitation of the CQDs, in a monolithic format suitable for a variety of applications including VLC.

2. Transfer printing on ultra-thin glass

μTP uses the reversible adhesion property of an elastomeric stamp to pick up semiconductor devices or structures from their growth substrate and transfer them to a non-native receiver substrate [7–9]. μTP has been demonstrated for the integration of III-V optoelectronic components with silicon circuitry [10] and for that of VCSELs, photodiodes and nanowire arrays with flexible polymer substrates [11, 12], amongst other uses. We recently reported TP of μLEDs with nano-scale printing resolution [13, 14] and we utilize the same basic approach here, for the μTP of μLEDs on ultra-thin glass. An array of 100 x 100 μm^2 InGaN μLEDs ready for μTP, suspended by sacrificial anchors after KOH under-etching, is initially fabricated [11] from a 2μm-thick LED epistructure grown on (111)-orientation silicon. A 6 x 6 array of these μLEDs is then printed directly onto a 30 μm-thick glass sheet (Schott AF32). Adhesion of the μLED to the glass is via van der Waals' bonding aided by liquid capillarity [15]. After μTP, an SU-8 electrical insulation layer is deposited and Ti/Au 50nm/200nm metal tracks are added to electrically address the μLEDs. Figures 1(a)-1(c) show photographs at progressively decreasing magnification of a 6 x 6 array of μLEDs printed onto flexible

Optics EXPRESS

glass containing the circuitry to address the full array (yield > 80%). The µLEDs can be seen in Fig. 1(a). As shown in Fig. 1(c) these arrays on thin glass are bendable. The µLEDs typically have a turn-on voltage around 3.5 V, as in Fig. 1(d), and achieve a forward-emitted optical power up to 16 µW, see Fig. 1(e). It is important to note that there is no heat sink other than the thin glass substrate, which explains this modest optical power. The current leakage seen before the turn-on voltage can be attributed to damage to the LED epistructure during the suspended LED fabrication. Figure 1(f) shows the spectral emission from these µLEDs measured straight through the thin glass. The main peak is at 460 nm and the shoulder at 470 nm is caused by a Fabry-Perot effect in the 2µm-thick epistructure.

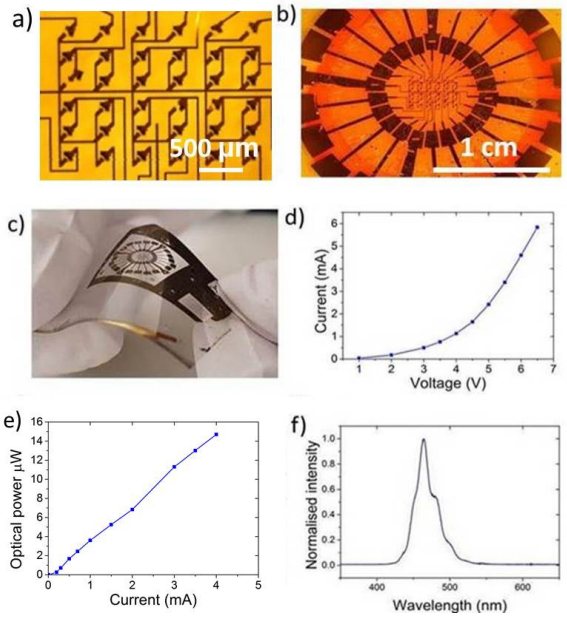

Fig. 1. a), b), c) Plan view photographs of a 6 x 6 array of µLEDs printed on thin glass with decreasing magnification. The µLEDs pictured here are 100 x 100 μm^2. A typical d) IV curve, e) LI curve and f) spectrum for these µLEDs at a drive current of 5 mA.

3. Integrated µLED/ color-converter device

A schematic of the full device with the CQDs integrated is shown in Fig. 2(a). It consists of blue µLEDs printed onto a first flexible glass sheet. This glass sheet is attached to a second glass sheet, already coated with a film of CQDs. For this, 12.5 µl of a 40 mg/ml solution of CQDs in toluene for the green sample and 30 mg/ml for the red and orange sample is drop coated onto the second thin glass sheet to coat a circular area of around 1 cm in diameter. The amount and concentration of the solution were tailored to absorb >95% of LED excitation light at 460 nm. The drop-coated CQD film is left to dry slowly, at a temperature of 5°C, to ensure uniformity. The thickness of the dried CQD film is typically a few µm. The CQDs are of the CdS_xSe_{1-x}/ZnS alloyed core/shell design and 6 nm in diameter (Cytodiagnostics). The emission wavelength is varied through the composition of the CdS_xSe_{1-x} core. We demonstrate conversion from the blue (µLED at 460 nm) to green (550 nm), orange (590 nm) and red (640 nm). The edges of the two glass sheets are sealed with a UV-curable epoxy (NOA65, Norland) and this assembly is all done in ambient conditions. A finalized device, fabricated with red CQDs, can be seen in Fig. 2(b). Close up images of the red, orange, and green devices taken from the top and with two µLEDs lit up, are shown in Fig. 2(c). As can be seen from Fig. 2(a) color-converted light is emitted through the second glass sheet and will be referred to as the 'forward' emitted light for the characterization in the rest of the paper.

Optics EXPRESS

Some of the light converted by the CQDs is however waveguided by the structure, both within the CQD film (refractive index n = 1.8) [16] and the thin glass sheets (n = 1.46). This is discussed in section 3.2.

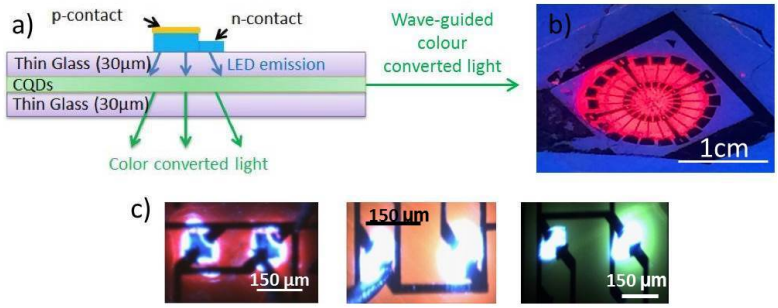

Fig. 2. a) Side view schematic of the integrated LED-color-converter device, b) oblique view of the red sample under UV illumination and c) images of the transfer printed LEDs lighting up on each of the three samples

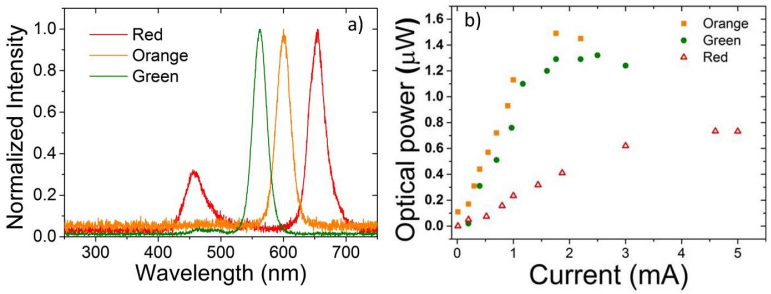

Fig. 3. a) Spectra of light emitted from the integrated LED-color-converter samples, and b) the respective optical power characteristics of the three samples

3.1 Spectra, absorption and efficiency

After µLED µTP and device metallisation, the devices are electrically probed and measured for spectral and light output power performance. Emission peaks at 640 nm, 590 nm and 550 nm for the red, orange and green sample respectively can be seen in Fig. 3(a). The smaller peak around 460 nm, seen most clearly for the red color-converter because of its relatively low optical power, is the spectral contribution from the unconverted blue light from the µLED. Absorption of µLED light is 95.5%, 97.5% and 99% for, respectively, the red, green and orange devices. These values are obtained by comparing the optical power of the color-converted and un-converted (blue) emissions from the three samples with the average optical power of the emission from µLEDs printed on a thin glass reference sample. The optical power of the color-converted light, vs. current from the µLED, from all three samples is seen in Fig. 3(b), and was measured using a Thorlabs power meter (PM100A) butt-coupled to the sample through a long-pass filter blocking unconverted blue light. The optical power at an injection current of 2 mA was 0.4 µW for the red device, 1.3 µW for the green device and 1.45 µW for the orange device. The rollover in the optical power seen in Fig. 3(b) is due to the thermal rollover of the µLEDs. Given the geometry of the structure, approximately 77% of the initial color converted photons are guided horizontally within the CQD layer and the flexible glass (see also section 3.2). However, as this light propagates it is reabsorbed [6] and re-emitted by the CQDs enabling to a certain extent guided photons to be recycled into the forward emission. Based on the structure geometry and ignoring scattering, 5% to 25% forward power efficiency can be expected for CQD quantum efficiency between 50% and 90%. The forward optical power conversion efficiency obtained here for the red, orange and

Optics EXPRESS

green color-converters, respectively, is 9%, 15% and 14%. The lower efficiency of the red device is attributed to a lower quantum yield. The forward power conversion efficiency is defined as the ratio of the optical power of the color-converted light to the optical power of the μLED taken on a reference sample minus the power of the un-converted blue light. Adding scattering and/or light extraction features in the structure should lead to higher forward conversion efficiency.

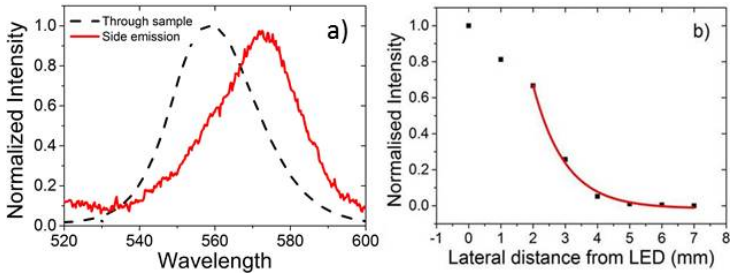

Fig. 4. a) Normalized spectra of the forward light emitted through the green CQD color-converter sample, and light emitted from the side of the sample at a distance of 1 cm away from the μLED. b) Light intensity as a function of lateral distance from the LED (taken in the forward direction i.e. through flexible glass)

3.2 Waveguiding

As represented in Fig. 2(a), the μLED emits light down through the glass and CQD layers. Because of the respective refractive indices of the CQDs and the flexible glass some color-converted light emitted outside the escape cone is guided horizontally through the CQD layer and the flexible glass. The waveguided emission was measured at the edge of the glass structure, 20 mm away from the μLED in this case. The corresponding spectrum is seen in the solid red line in Fig. 4(a). It is red-shifted because of self-absorption, when compared to the forward emission as illustrated in the dashed black line in Fig. 4(a) by 3 nm for the red sample, 5 nm for the orange sample and 10 nm for the green sample. The waveguided loss was also measured by translating a spectrometer in parallel to the surface of the glass, and registering the relative forward emitted intensity with respect to the distance from the μLED position. This loss is a combination of scattering and of self-absorption with some absorbed photons reemitted in the escape cone. Figure 4(b) shows the forward intensity at 555 nm versus the lateral distance from the edge of LED excitation for the green sample. When the distance from the LED is large enough so that the forward light and leaky modes are not significantly coupled into the detector, the intensity decays exponentially. The loss can be extracted by fitting the data (red line in Fig. 4(b)). The guiding loss is 1.50 cm^{-1}, 0.97 cm^{-1} and 1.05 cm^{-1} for the red (642 nm), orange (594 nm), and green (558 nm) device respectively, taken at the peak wavelength measured directly under the μLED. The higher loss for the red device is consistent with the lower quantum efficiency for the red CQDs.

4. VLC demonstration

The devices were demonstrated for VLC as shown in Figs. 5(a) and 5(b). The devices were driven with a DC signal (drive current, 3 mA, chosen to maximise the optical power during data transmission without damaging the μLEDs) combined through a bias-T with a modulated, OFDM signal. For this, an incoming stream of bits was encoded using multi-level quadrature (M -QAM) before a Hermitian symmetry and fast Fourier transformation (FFT) operation was applied on N_{FFT} M -QAM symbols. Here N_{FFT} = 1024. The resulting OFDM stream was transmitted to the μLED through an arbitrary waveform generator, Agilent 81180A. Bit and power loading was used. The device was placed directly onto the top of a compound parabolic condenser lens (approximately 4 cm in length), and the modulated light collected at the bottom of the lens (back-to-back) with an avalanche photodiode (Hamamatsu

Optics EXPRESS

S8664-50K). The detected signal was then sent to an oscilloscope (MS07104B) and demodulated offline. The optical data rates were measured for the three devices considering a bit error rate (BER) of 3.8×10^{-3}, which is the error-free limit assuming forward error correction (FEC) is implemented. Data rates of 46 Mbps, 44 Mbps, and 61 Mbps for, respectively, the red, orange and green device, were obtained in these conditions, Fig. 5(c). The higher data rate obtained for the green device is due to the higher contribution of unabsorbed µLED light compared to the orange device (2.5% versus <1% for the orange) and to a higher efficiency compared to the red device.

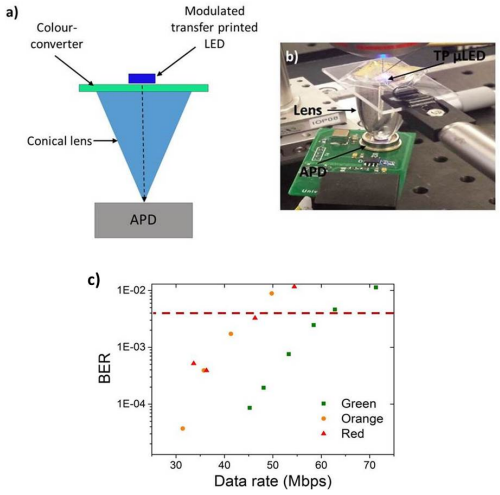

Fig. 5. The setup used for the acquisition of data transmission rates for the integrated color-converters. Shown a) schematically and b) in a photograph. c) Data rates for the red, orange and green CQD color-converting samples.

5. Conclusion

In this work, we have demonstrated a novel integrated format of color-converted light source, which has potential for a range of applications. We have done this by integrating, through a µTP process, an ultra-thin blue-emitting InGaN LED with an ultra-thin glass platform functionally enhanced with CQD color-converters. Once fully contacted, these red, orange and green hybrid LED-color-converter devices achieve forward power conversion efficiencies of, respectively, 9%, 15% and 14%. We have demonstrated, for the first time, the potential for these integrated LED-color-converter devices for VLC applications, with data rates of 46 Mbps, 44 Mbps and 61 Mbps for the red, orange and green samples respectively. The wavelength division multiplexing (WDM) capacity of these samples would therefore be close to 151 Mbps. The performance of these devices is currently limited in terms of emitted power because of the low thermal conductivity of glass, but significant enhancement is expected by implementing a thermal management structure on the contact side of the LEDs.

Supporting data can be found at DOI: 10.15129/7e192c6b-a4c8-445f-8dde-68948ec850cc.

Funding

EPSRC grant EP/K00042X/1. DJ Wallis also acknowledges the support of EPSRC grant EP/N01202X/1.